PROCEEDINGS OF SCIENCE

Searching for odderon exchange in exclusive $pp \to pp\phi$ and $pp \to pp\phi\phi$ reactions at the LHC

P. Lebiedowicz,[a,*] **O. Nachtmann**[b] **and A. Szczurek**[a,†]

[a] *Institute of Nuclear Physics Polish Academy of Sciences, Radzikowskiego 152, PL-31342 Kraków, Poland*

[b] *Institut für Theoretische Physik, Universität Heidelberg, Philosophenweg 16, D-69120 Heidelberg, Germany*

E-mail: Piotr.Lebiedowicz@ifj.edu.pl, O.Nachtmann@thphys.uni-heidelberg.de, Antoni.Szczurek@ifj.edu.pl

The possibility to use the exclusive $pp \to pp\phi$ and $pp \to pp\phi\phi$ reactions in identifying the odderon exchange is discussed. So far there is no unambiguous experimental evidence for the odderon, the charge conjugation $C = -1$ counterpart of the $C = +1$ pomeron. Recently proposed tensor-pomeron and vector-odderon model for soft high-energy reactions is applied. For the $pp \to pp\phi$ reaction at high energies the photon-pomeron fusion is the dominant process and the odderon-pomeron fusion is an interesting alternative. Adding odderon exchange improves considerably description of the proton-proton angular correlations measured by the WA102 collaboration. The $pp \to pp\phi\phi$ process via pomeron-pomeron fusion is advantageous one as here the odderon does not couple to protons. The observation of large $M_{\phi\phi}$ and the rapidity difference $Y_{\phi\phi}$ seems well suited to identify odderon exchange. Comparisons with data from the WA102 experiment are made and predictions for LHC experiments are given.

40th International Conference on High Energy physics - ICHEP2020
July 28 - August 6, 2020
Prague, Czech Republic (virtual meeting)

[*] Speaker
[†] Also at *College of Natural Sciences, Institute of Physics, University of Rzeszów, Pigonia 1, PL-35310 Rzeszów, Poland.*

PoS(ICHEP2020)477

1. Introduction

The odderon was introduced on theoretical grounds in [1]. It was predicted in QCD as a colourless charge-conjugation C-odd three-gluon bound state exchange [2, 3]. Recent experimental results by the TOTEM Collaboration [4, 5] have brought the odderon question in proton-proton elastic scattering to the forefront again. It is of great importance to study possible odderon effects in other reactions. As was discussed in [6] exclusive diffractive J/ψ and ϕ production from the pomeron-odderon fusion in high-energy pp and $p\bar{p}$ collisions is a direct probe for a possible odderon exchange. We shall argue here that the central exclusive production (CEP) of a $\phi\phi$ state offers a very nice way to look for odderon effects as suggested in [7].

In this contribution we will be concerned with CEP of single and double $\phi(1020)$ meson production observed in the K^+K^- or $\mu^+\mu^-$ channels in pp collisions as a possible source of information for soft odderon exchange (see figure 1). The presentation is based on [8] where all details and many more results can be found. At high energies the $pp \to pp\phi$ reaction should be mainly due to photon-pomeron exchange. The odderon-pomeron fusion mechanism is an interesting alternative. The $pp \to pp\phi\phi$ reaction should be mainly due to double-pomeron exchange with resonant production at low $\phi\phi$ invariant masses and the continuum processes (reggeized-ϕ-meson and odderon exchanges) at higher $M_{\phi\phi}$. The process with an intermediate $\hat{t}/\hat{u}$-channel odderon exchange ($\mathbb{P}$-$\mathbb{O}$-$\mathbb{P}$) is a good candidate for the odderon searches, as it does not involve the coupling of the odderon to the proton.

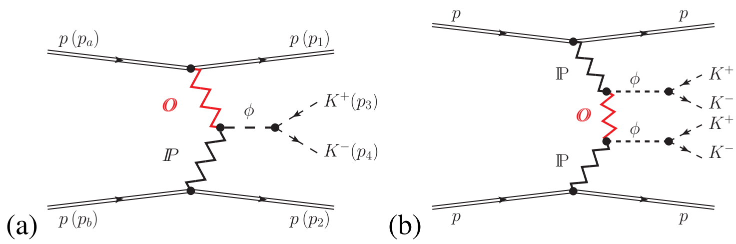

Figure 1: Diagrams for (a) single ϕ production and for (b) double ϕ production with odderon ($\mathbb{O}$) exchange. There are also diagrams with the rôle of the protons interchanged, $(p\,(p_a), p\,(p_1)) \leftrightarrow (p\,(p_b), p\,(p_2))$.

We treat our reactions in the tensor-pomeron and vector-odderon approach as introduced in [9]. This approach has a good basis from nonperturbative QCD using functional integral techniques [10]. We describe the pomeron and the $C = +1$ reggeons as effective rank 2 symmetric tensor exchanges, the odderon and $C = -1$ reggeons as effective vector exchanges. There are by now many applications of the tensor-pomeron model to two-body hadronic reactions [11], to photoproduction, to DIS structure functions at low x, and especially to CEP reactions: $p + p \to p + X + p$, where $X = \eta, \eta', f_0, f_1, f_2, \pi^+\pi^-, p\bar{p}, K\bar{K}, 4\pi, 4K, \rho^0, \phi, \phi\phi$; see e.g. [8, 12–15].

2. A sketch of formalism

As an example, we consider the reaction

$$p(p_a) + p(p_b) \to p(p_1) + [\phi(p_{34}) \to K^+(p_3) + K^-(p_4)] + p(p_2), \tag{1}$$

where $p_{a,b}$, $p_{1,2}$ denote the four-momenta of the protons and $p_{3,4}$ denote the four-momenta of the K mesons, respectively. For high energies and central ϕ production we expect the reaction (1) to be dominated by the fusion processes $\gamma\mathbb{P} \to \phi$ and $\mathbb{O}\mathbb{P} \to \phi$. For the first process all couplings are, in essence, known. The parameters of ϕ photoproduction were fixed to describe the HERA data taking into account the ϕ-ω mixing effect [8]. For the odderon-exchange process we shall use the ansätze from [9] and we shall try to get information on the odderon parameters and couplings from the comparison to the WA102 data for the $pp \to pp\phi$ and $pp \to pp\phi\phi$ reactions. Of course, at the relatively low c.m. energy of the WA102 experiment, $\sqrt{s} = 29.1$ GeV, we have to include also subleading contributions with reggeized-vector-meson (or reggeon) exchanges discussed in [8].

The Born-level amplitude for the diffractive production of the $\phi(1020)$ via odderon-pomeron fusion [figure 1(a)] can be written as

$$\begin{aligned}\mathcal{M}^{(\mathbb{O}\mathbb{P})}_{pp\to ppK^+K^-} &= (-i)\bar{u}(p_1,\lambda_1) i\Gamma^{(\mathbb{O}pp)}_{\mu}(p_1,p_a)u(p_a,\lambda_a)\, i\Delta^{(\mathbb{O})\,\mu\rho_1}(s_1,t_1)\, i\Gamma^{(\mathbb{P}\mathbb{O}\phi)}_{\rho_1\rho_2\alpha\beta}(-q_1,p_{34}) \\ &\times i\Delta^{(\phi)\,\rho_2\kappa}(p_{34})\, i\Gamma^{(\phi KK)}_{\kappa}(p_3,p_4)\, i\Delta^{(\mathbb{P})\,\alpha\beta,\delta\eta}(s_2,t_2)\,\bar{u}(p_2,\lambda_2) i\Gamma^{(\mathbb{P}pp)}_{\delta\eta}(p_2,p_b)u(p_b,\lambda_b)\,. \quad (2)\end{aligned}$$

The kinematic variables are $p_{34} = p_3 + p_4$, $q_1 = p_a - p_1$, $q_2 = p_b - p_2$, $t_1 = q_1^2$, $t_2 = q_2^2$, $s = (p_a + p_b)^2$, $s_1 = (p_1 + p_{34})^2$, $s_2 = (p_2 + p_{34})^2$. The effective pomeron propagator and the pomeron-proton vertex function are as follows [9]:

$$i\Delta^{(\mathbb{P})}_{\mu\nu,\kappa\lambda}(s,t) = \frac{1}{4s}\left(g_{\mu\kappa}g_{\nu\lambda} + g_{\mu\lambda}g_{\nu\kappa} - \frac{1}{2}g_{\mu\nu}g_{\kappa\lambda}\right)(-is\alpha'_{\mathbb{P}})^{\alpha_{\mathbb{P}}(t)-1}\,, \quad (3)$$

$$i\Gamma^{(\mathbb{P}pp)}_{\mu\nu}(p',p) = -i3\beta_{\mathbb{P}NN}F_1((p'-p)^2)\left\{\frac{1}{2}\left[\gamma_\mu(p'+p)_\nu + \gamma_\nu(p'+p)_\mu\right] - \frac{1}{4}g_{\mu\nu}(\not{p}'+\not{p})\right\}, \quad (4)$$

where $\beta_{\mathbb{P}NN} = 1.87$ GeV^{-1} and $t = (p'-p)^2$. For simplicity we use the electromagnetic Dirac form factor $F_1(t)$ of the proton. The pomeron trajectory $\alpha_{\mathbb{P}}(t)$ is assumed to be of standard linear form: $\alpha_{\mathbb{P}}(t) = \alpha_{\mathbb{P}}(0) + \alpha'_{\mathbb{P}}\,t$, with $\alpha_{\mathbb{P}}(0) = 1.0808$ and $\alpha'_{\mathbb{P}} = 0.25$ GeV^{-2}.

Our ansatz for the $C = -1$ odderon follows (3.16), (3.17) and (3.68), (3.69) of [9]:

$$i\Delta^{(\mathbb{O})}_{\mu\nu}(s,t) = -ig_{\mu\nu}\frac{\eta_{\mathbb{O}}}{M_0^2}(-is\alpha'_{\mathbb{O}})^{\alpha_{\mathbb{O}}(t)-1}\,, \quad (5)$$

$$i\Gamma^{(\mathbb{O}pp)}_{\mu}(p',p) = -i3\beta_{\mathbb{O}pp}\,M_0\,F_1((p'-p)^2)\,\gamma_\mu\,, \quad (6)$$

where $\eta_{\mathbb{O}}$ is a parameter with value $\eta_{\mathbb{O}} = \pm 1$; $M_0 = 1$ GeV is inserted for dimensional reasons. We assumed $\beta_{\mathbb{O}pp} = 0.1 \times \beta_{\mathbb{P}NN}$. We take $\alpha_{\mathbb{O}}(t) = \alpha_{\mathbb{O}}(0) + \alpha'_{\mathbb{O}}\,t$. In our calculations we shall choose as default values $\alpha_{\mathbb{O}}(0) = 1.05$, $\alpha'_{\mathbb{O}} = 0.25\,$GeV^{-2}, and $\eta_{\mathbb{O}} = -1$; see [8].

For the $\mathbb{P}\mathbb{O}\phi$ vertex we use an ansatz analogous to the $\mathbb{P}\phi\phi$ vertex (see (3.48)–(3.50) of [14])

$$\begin{aligned}i\Gamma^{(\mathbb{P}\mathbb{O}\phi)}_{\rho_1\rho_2\alpha\beta}(-q_1,p_{34}) &= i\left[2\,a_{\mathbb{P}\mathbb{O}\phi}\,\Gamma^{(0)}_{\rho_2\rho_1\alpha\beta}(p_{34},-q_1) - b_{\mathbb{P}\mathbb{O}\phi}\,\Gamma^{(2)}_{\rho_2\rho_1\alpha\beta}(p_{34},-q_1)\right] \\ &\times F_M(q_2^2)\,F_M(q_1^2)\,F^{(\phi)}(p_{34}^2)\,. \quad (7)\end{aligned}$$

Here we use the relations (3.20) of [9] and as in (3.49) of [14] we take the factorised form for the $\mathbb{P}\mathbb{O}\phi$ form factor; see [8]. The coupling parameters $a_{\mathbb{P}\mathbb{O}\phi}$, $b_{\mathbb{P}\mathbb{O}\phi}$ in (7) and the cut-off parameter $\Lambda^2_{0,\,\mathbb{P}\mathbb{O}\phi}$ in $F_M(t) = 1/(1 - t/\Lambda^2_{0,\,\mathbb{P}\mathbb{O}\phi})$ could be adjusted to experimental data. The WA102 data allow us to determine the respective coupling constants as $a_{\mathbb{P}\mathbb{O}\phi} = -0.8$ GeV^{-3}, $b_{\mathbb{P}\mathbb{O}\phi} = 1.6$ GeV^{-1}, and $\Lambda^2_{0,\,\mathbb{P}\mathbb{O}\phi} = 0.5$ GeV^2[8]. We have checked that these parameters are compatible with our analysis of the WA102 data for the $pp \to pp\phi\phi$ reaction in [14].

The full amplitude includes the pp-rescattering corrections in the eikonal approximation; see [8].

3. Results

It is very difficult to describe the WA102 data from [16] for the $pp \to pp\phi$ reaction including the $\gamma\mathbb{P}$-fusion mechanism only. As was presented in [8] inclusion of the odderon-exchange contribution significantly improves the description of the pp azimuthal correlations (ϕ_{pp} is angle between the transverse momentum vectors $\boldsymbol{p_{t,1}}$, $\boldsymbol{p_{t,2}}$ of the outgoing protons) and the $\mathrm{dP_t} = |\boldsymbol{p_{t,2}} - \boldsymbol{p_{t,1}}|$ dependence of ϕ CEP measured by the WA102 collaboration. The absorption effects - very important - were included in the calculations. In the left panel of figure 2 we present the $\mathbb{O}$-$\mathbb{P}$ contribution (approach II of [8]) together with the γ-$\mathbb{P}$ contribution and with the subleading terms. Adding odderon exchange term improves description of the proton-proton angular correlations. Having fixed the parameters of our model to the WA102 data we show our predictions at $\sqrt{s} = 13$ TeV for the LHC. Here we focus on the limited invariant mass region around the $\phi(1020)$ resonance.

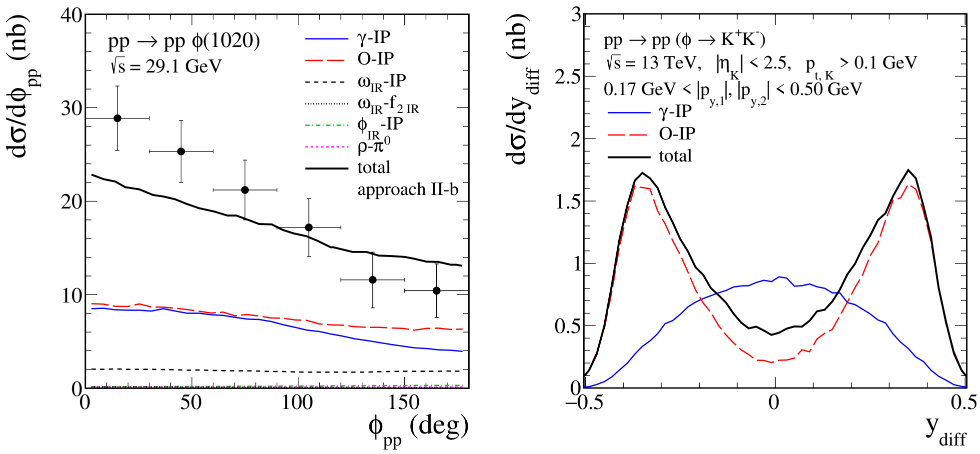

Figure 2: Left panel: The distributions in ϕ_{pp} together with the WA102 experimental data points for $\sqrt{s} = 29.1$ GeV normalized to the central value of the total cross section $\sigma_{\rm exp} = 60$ nb from [16]. The coherent sum of all terms is shown by the black solid line. Right panel: The distribution in rapidity difference between kaons for the $pp \to pp(\phi \to K^+K^-)$ reaction for the ATLAS-ALFA kinematics.

In the right panel of figure 2 we show the results for the $pp \to pp(\phi \to K^+K^-)$ reaction for experimental conditions relevant for ATLAS-ALFA or CMS-TOTEM. The $\mathbb{O}$-$\mathbb{P}$ contribution dominates at larger p_{t,K^+K^-} (or transverse momentum of the K^+K^- pair) and $|\mathrm{y_{diff}}|$ compared to the γ-$\mathbb{P}$ contribution. For the ATLAS-ALFA kinematics the absorption effects lead to a large damping of the cross sections for both the mechanisms; see Table II of [8].

Now we discuss the $pp \to pp\mu^+\mu^-$ reaction at forward rapidities and without measurement of protons relevant for LHCb. Figure 3 shows the distribution in transverse momentum of the $\mu^+\mu^-$ pair. We can see that the low-$p_{t,\mu^+\mu^-}$ cut can be helpful to reduce the dimuon-continuum and γ-$\mathbb{P}$-fusion contributions. In the right panel we show the $\mathrm{y_{diff}}$ (rapidity difference between muons) distribution when imposing in addition a cut $p_{t,\mu^+\mu^-} > 0.8$ GeV. The $\gamma\gamma \to \mu^+\mu^-$ continuum contribution is now very small. At $\mathrm{y_{diff}} = 0$ the $\mathbb{O}$-$\mathbb{P}$ term should win with the γ-$\mathbb{P}$ term. In contrast to dikaon CEP here there is for both contributions a maximum at $\mathrm{y_{diff}} = 0$.

Now we go to the $pp \to pp\phi\phi$ reaction. Figure 4 shows the results including the $f_2(2340)$ term and the continuum processes due to reggeized-ϕ and odderon exchanges. For the details how to calculate these processes see [14]. Inclusion of the odderon exchange improves the description

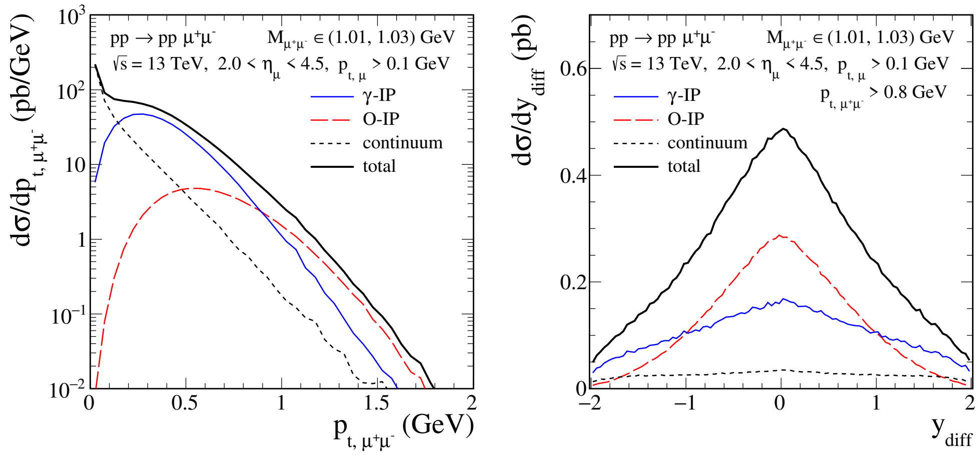

Figure 3: The distributions in transverse momentum of the $\mu^+\mu^-$ pair (left) and in rapidity difference between muons (right) for the $pp \to pp\mu^+\mu^-$ reaction for $\sqrt{s}$ = 13 TeV and $M_{\mu^+\mu^-} \in (1.01, 1.03)$ GeV. Results for the γ-$\mathbb{P}$ and $\mathbb{O}$-$\mathbb{P}$ fusion terms, the continuum term as well as their coherent sum are shown.

of the WA102 data [17] for the $pp \to pp\phi\phi$ reaction; see the left panel of figure 4. Here we showed results for the odderon-exchange contribution with the parameters of our model fixed to the WA102 data [16] on single CEP of ϕ; see section IV A of [8]. In the right panel we show the distribution in four-kaon invariant mass for the LHCb experimental conditions. The small intercept of the ϕ-reggeon exchange, $\alpha_\phi(0) = 0.1$ makes the ϕ-exchange contribution steeply falling with increasing M_{4K}. Therefore, an odderon with an intercept $\alpha_{\mathbb{O}}(0)$ around 1.0 should be clearly visible in the region of large M_{4K} (and also for large rapidity distance between the ϕ mesons).

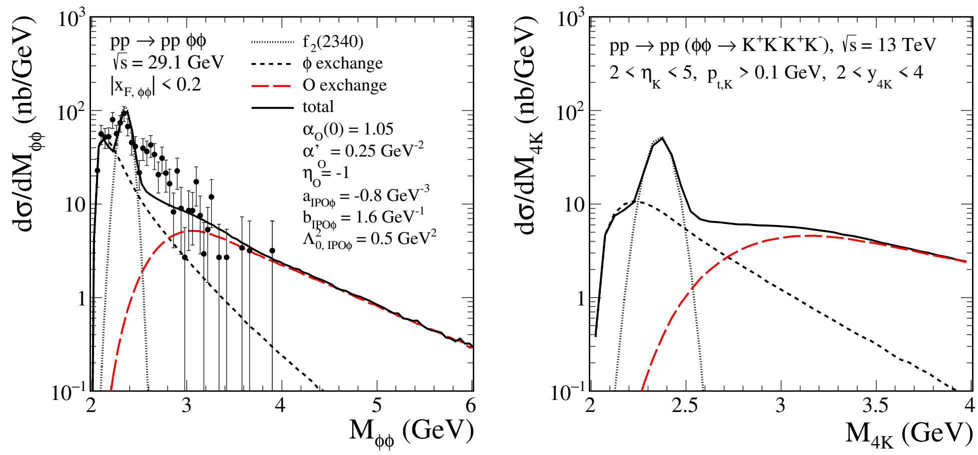

Figure 4: The distributions in $\phi\phi$ invariant mass (left) for $\sqrt{s}$ = 29.1 GeV together with the WA102 data from [17] and (right) in M_{4K} for the LHCb kinematics. The short-dashed line corresponds to the reggeized-ϕ-exchange contribution, the dotted line corresponds to the $f_2(2340)$ contribution, the red long-dashed line represents the $\mathbb{O}$-exchange contribution. The coherent sum of all terms is shown by the black solid line.

4. Conclusions

We have discussed in detail the $pp \to pp\phi$ and $pp \to pp\phi\phi$ reactions. For single ϕ CEP at the LHC there are two basic processes: the relatively well known γ-$\mathbb{P}$ fusion and the rather elusive $\mathbb{O}$-$\mathbb{P}$ fusion. We fixed the parameters of the pomeron-odderon contribution to obtain a good description of the WA102 data [16, 17]. Then we have estimated the integrated cross sections and several differential distributions at the LHC; see Table II of [8]. It is a main result of our analysis that, the $y_{\rm diff}$ distributions are very different for the γ-$\mathbb{P}$- and $\mathbb{O}$-$\mathbb{P}$-fusion processes. The $\mu^+\mu^-$ channel seems to be less promising in identifying the odderon exchange at least when only the $p_{t,\mu}$ cuts are imposed. To observe a sizeable deviation from photoproduction a $p_{t,\mu^+\mu^-} > 0.8$ GeV cut on the transverse momentum of the $\mu^+\mu^-$ pair seems necessary. A combined analysis of both the K^+K^- and the $\mu^+\mu^-$ channels should be the ultimate goal in searches for odderon exchange.

The $pp \to pp\phi\phi$ process via odderon exchange [figure 1(b)] seems promising as here the odderon does not couple to protons. We find from our model that the odderon-exchange contribution should be distinguishable from other contributions for relatively large four-kaon invariant masses (outside of the region of resonances) and for large rapidity distance between the ϕ mesons. Hence, to study this type of mechanism one should investigate "three-gap events" (proton–gap–ϕ–gap–ϕ–gap–proton). Experimentally, this should be a clear signature.

We are looking forward to first experimental results on single and double ϕ CEP at the LHC.

Acknowledgments

The authors thank the organisers of the ICHEP 2020 conference for making this presentation of our results possible. This work was partially supported by the NCN Grant No. 2018/31/B/ST2/03537.

References

[1] L. Łukaszuk and B. Nicolescu, *Lett. Nuovo Cim.* **8** (1973) 405.
[2] J. Kwieciński and M. Praszałowicz, *Phys. Lett. B* **94** (1980) 413.
[3] J. Bartels, *Nucl. Phys. B* **175** (1980) 365.
[4] G. Antchev *et al.*, (TOTEM Collaboration), *Eur. Phys. J. C* **79** (2019) 785.
[5] G. Antchev *et al.*, (TOTEM Collaboration), *Eur. Phys. J. C* **80** (2020) 91.
[6] A. Schäfer, L. Mankiewicz, and O. Nachtmann, *Phys. Lett. B* **272** (1991) 419.
[7] C. Ewerz, arXiv:hep-ph/0306137 [hep-ph].
[8] P. Lebiedowicz, O. Nachtmann, and A. Szczurek, *Phys. Rev. D* **101** (2020) 094012.
[9] C. Ewerz, M. Maniatis, and O. Nachtmann, *Annals Phys.* **342** (2014) 31.
[10] O. Nachtmann, *Annals Phys.* **209** (1991) 436.
[11] C. Ewerz, P. Lebiedowicz, O. Nachtmann, and A. Szczurek, *Phys. Lett. B* **763** (2016) 382.
[12] P. Lebiedowicz, O. Nachtmann, and A. Szczurek, *Annals Phys.* **344** (2014) 301.
[13] P. Lebiedowicz, O. Nachtmann, and A. Szczurek, *Phys. Rev. D* **93** (2016) 054015.
[14] P. Lebiedowicz, O. Nachtmann, and A. Szczurek, *Phys. Rev. D* **99** (2019) 094034.
[15] P. Lebiedowicz, J. Leutgeb, O. Nachtmann, A. Rebhan, and A. Szczurek, *Phys. Rev. D* **102** (2020) 114003.
[16] A. Kirk, *Phys. Lett. B* **489** (2000) 29.
[17] D. Barberis *et al.*, (WA102 Collaboration), *Phys. Lett. B* **432** (1998) 436.